where P is proportional to the battery capacity. This variant resembles case 1, except that the battery capacity, rather than the propellant reserve, is taken into account; i.e., the optimal φ providing the maximum of $\bar{M}$ also has a technical significance here.

3) Gas jets plus, flywheel, stabilization system powered by solar battery. In this case,

$$\bar{M} = (dM/dt)/N \tag{29}$$

where dM/dt is the data transmission rate;

$$dM/dt = C/(B_3/N + \delta)^2$$

N is the average power obtained from the solar cells to maintain orientation;

$$N = B_3/\varphi$$

and B_3 is a parameter depending on the vehicle and flywheel moments of inertia as well as on characteristics of the orientation and power supply systems. In this case a quest for maximum $\bar{M}$ by choice of the optimal φ has no technical significance, because dM/dt increases as long as φ decreases (N increases). Thus, as in the first case at τ = constant, it is expedient to take the minimum allowable value φ determined by the technical capabilities of the orientation system or by the limiting capabilities of the solar battery (weight or area). The optimal parabolic antenna for this value of φ will provide maximum D and maximum M under the given limitations.

Flight Measurement of Aerodynamic Coefficients on a Bomb

Neil Edmund Gilbert*
Weapons Research Establishment, Salisbury, South Australia

Nomenclature

c_1 to c_8 = least-squares coefficients
C_m,C_n = static normal and side moment coefficients, respectively
C_Z,C_Y = static normal and side force coefficients, respectively
M = Mach number
$OXYZ$ = bomb body axes
p,q,r = angular velocity components
t = time from release
α,β = angle of pitch and yaw, respectively
θ = total angle of incidence
ϕ = angular orientation of body relative to plane of incidence; $\tan\phi = \tan\beta/\tan\alpha$

Introduction

A JOINT research program was initiated in 1960 by the Royal Aircraft Establishment (RAE) in the United Kingdom and the Weapons Research Establishment (WRE) in Australia to study the ballistic performance of bombs stabilized by fixed cruciform fins.[1] The program was extended in 1964 in the United States on a tripartite basis in collaboration with the Naval Ordnance Laboratory (NOL) in order to deal with bombs stabilized by split skirts and freely spinning tails.[2-4] To complete the program, two bombs stabilized by fixed cruciform fins were dropped during 1968 to study two types of flight instability, namely catastrophic yaw and Magnus instability.

Received June 22, 1970; revision received September 15, 1970.
* Member of Flight Research Group, Aerospace Division; presently at La Trobe University, Victoria, Australia.

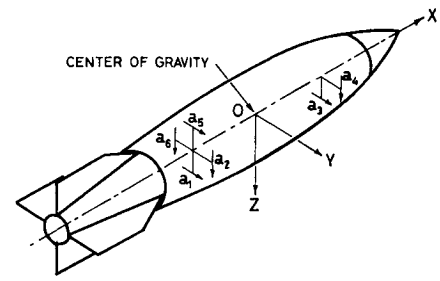

Fig. 1 Positions on bomb of six-linear accelerometers.

An aim of the program has been to determine the aerodynamic stability coefficients as a function of M, θ, and ϕ. A convenient mathematical model of the forces and moments, which makes use of the properties of rotational and reflectional symmetry of a vehicle with fins, has been developed by Maple and Synge.[5] The present Note describes the derivation of aerodynamic force and moment coefficients on the M823 research store using the Maple and Synge theory, and is based on three Technical Notes[6-8] which supply more detail as well as the computer program used. Because of insufficient instrumentation and inaccurate data, the axial forces and moments could not be analysed, so that only lateral force and moment coefficients are derived. The method has been applied to bombs stabilized by split skirts and freely spinning monoplane and cruciform tails, but is here confined to bombs stabilized by fixed cruciform fins, and results are given only for the catastrophic yaw experiment.

Instrumentation

The Euler equations of motion show the various quantities required in order to determine the aerodynamic forces and moments.[9] Ground cameras together with meteorological data provided the necessary trajectory data. Given the mass and moments of inertia of the bomb, the problem was to select and position instruments on the bomb which would most easily and accurately record the required quantities using a telemetry system.[6]

The instruments fitted were a differential pressure incidence meter to obtain α and β, four laterally positioned linear accelerometers, three rate gyroscopes with mutually perpendicular axes (one along OX in Fig. 1), and a strain gauge mounted in the tail section to record roll torque. This selection would enable a comparison of forces and moments derived using various combinations of instrument measurements. Good agreement would serve to verify the reliability of these measurements. A longitudinally positioned accelerometer was not fitted because previous experiments proved unsuccessful.

By differentiating incidence meter measurements, pitch and yaw rates q and r were derived as an alternative to direct measurement by rate gyroscopes. Linear accelerometers were used both directly to give the forces and indirectly for deriving angular accelerations $\dot{q}$ and $\dot{r}$, thus providing an alternative to differentiated rate gyroscope measurements. To derive the forces and moments without using rate gyroscopes, at least five and preferably six suitably positioned linear accelerometers were required (labelled a_1 to a_6 on Fig. 1). On the vehicle being studied, a_5 and a_6 were omitted, but by using an iterative approximation procedure,[6] the lateral forces and moments could be derived. Because roll acceleration $\dot{p}$ could not be obtained to sufficient accuracy from either the strain gauge, ground cameras, or appropriate rate gyroscope, the axial moments could not be analysed.

Mathematical Model

Dependence of the derived aerodynamic forces and moments upon θ, ϕ, and p, q, and r is determined by fitting the

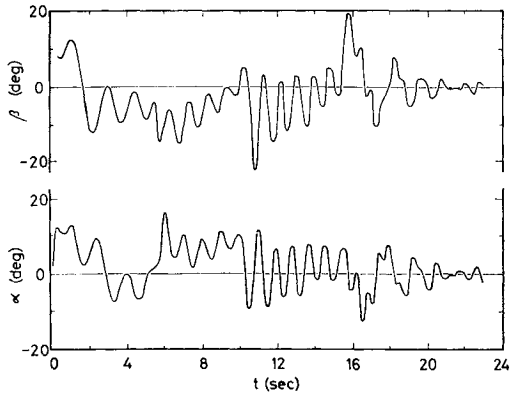

Fig. 2 α and β vs t.

flight data to a mathematical model of the force and moment system developed by Maple and Synge.[5] Reference 6 describes in detail the derivation of suitable models as well as the assumptions made and the limitations.

The total lateral force and moment coefficients are divided into static and dynamic components, the dynamic consisting of both Magnus and damping coefficients. Expansions for these components may be written in the form of a power series in $\tan\theta$ which must be truncated at some point.[7] The magnitude of the component coefficient relative to the total coefficient and the resulting agreement with wind-tunnel data are used in choosing the power series for each component.

The static lateral force and moment coefficients may be divided into normal and side components with respect to the plane of incidence. The static normal force and moment coefficients are defined by similar expansions of the form,†

$$c_1 \tan\theta + [c_2 + c_3 \cos 4\phi] \tan^3\theta + [c_4 + (c_5 + c_6) \cos 4\phi] \tan^5\theta$$

and the corresponding side coefficients by

$$c_3 \sin 4\phi \tan^3\theta + (c_5 - c_6) \sin^4\phi \tan^5\theta$$

The Magnus force or roll dependent force, which is assumed to be normal to the plane of incidence, is in the same direction as the static side force and is in general smaller in magnitude. The Magnus force and moment are defined by $c_7 \tan\theta$.

The damping force and moment coefficients may be divided into pitching and yawing components with respect to the body axes. As with Magnus components, the order in magnitude is very small compared with the static components. Assuming that the pitch and yaw damping coefficients are linearly dependent upon q and r, respectively, the damping coefficient derivatives are defined simply by c_8.

Finally, zero error terms in the static coefficients are introduced into the model. They may be attributed to either an asymmetrical flow caused possibly by geometrical misalignments in the test vehicle, offset zero levels in the instrumentation, or extrapolation of the total coefficients to zero incidence. When roll lock-in occurs, the minimum value of θ experienced is often large. Then, if large zero errors are obtained, these may be attributed mainly to the last source. If, by including and excluding zero errors from the model, a large difference is observed in the derived aerodynamic coefficients, then it may be difficult to obtain reliable results.

Suitable Flight Regions

A valid representation of the force and moment system can only be achieved for the range of angle of incidence

† The coefficients c_1 to c_8 are functions of M and p, but p equals zero except for c_7. They are assumed constant throughout a selected region of data and are determined using the least-squares criterion.

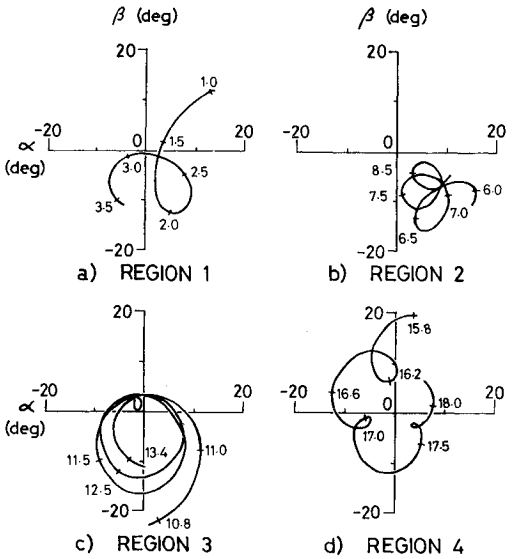

Fig. 3 α and β for analyzed flight regions. Numbers beside tick marks indicate time t, sec.

experienced during the period over which the analysis is performed. Bonkers, or lateral pulse rockets, were fitted to the bomb being studied so that a large incidence range could be achieved later in the flight as well as following release. The three bonkers fitted were fired ~5, 10, and 15 sec following release. The variation of α and β with time from release t for the first 23 sec of flight is given in Fig. 2. Periods of large amplitude motion may be observed to have occurred following each disturbance. A region of the data following each disturbance was selected such that two or three complete cycles of θ took place, as this was found to considerably reduce the effect of bias errors in the incidence meter and accelerometers. For low roll rates, a complete number of cycles of ϕ is also very important in reducing bias errors. Figure 3 shows polar plots of α and β throughout the four regions, and ϕ is given by β/α for the small values experienced. Whereas regions 3 and 4 traced through three and almost one complete cycle of ϕ, respectively, regions 1 and 2 each traced through less than a complete cycle. Bias errors may therefore be expected to be less effectively reduced in regions 1 and 2.

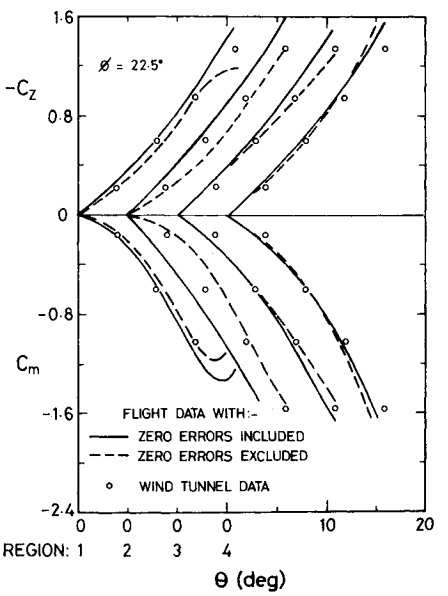

Fig. 4 Effect of zero errors in free-flight data, C_Z and C_m vs θ.

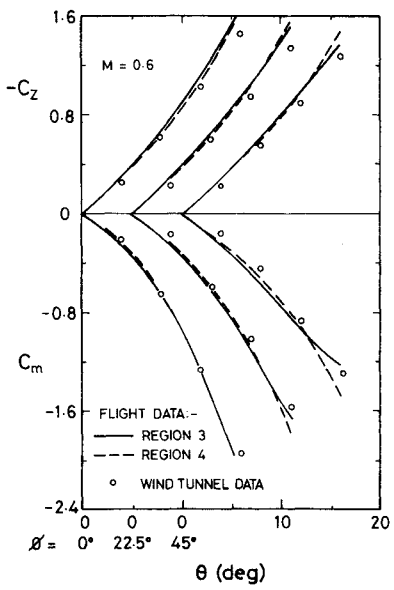

Fig. 5 Comparison of wind-tunnel and free-flight data, C_Z and C_m vs θ.

Results

To test the reliability of results obtained for each region, aerodynamic coefficients derived by both including and excluding zero errors from the model were compared (see Fig. 4). Because of the large differences observed for region 2, it is concluded that large bias errors are present, thus rendering region 2 unsuitable for analysis. Although for region 1 the difference is smaller but significant, results appear unrealistic towards the higher values of the incidence range so that region 1 is also considered unsuitable for analysis. Further results are thus confined to regions 3 and 4. Because M and p remained fairly constant throughout these two regions, results can be compared between regions as well as with wind-tunnel data.

Very good agreement was observed for values of q and r derived using incidence meter measurements with those obtained from rate gyroscopes. This served to verify the rate gyroscope measurements and to show that q and r could be successfully derived using incidence meter measurements, though not quite as accurately. Also, very good agreement was observed for values of $\dot{q}$ and $\dot{r}$ derived from gyroscopes with those derived from accelerometers. The total aerodynamic forces and moments may therefore be determined using rate gyroscopes to replace two-linear accelerometers without any significant loss in accuracy.

Aerodynamic coefficients were derived using accelerometers only, rate gyroscopes and four accelerometers, and rate gyroscopes with all four possible combinations of two accelerometers. The agreement of static force and moment coefficients derived using each instrument combination was very good, with results generally within 0.02 for the normal and side force coefficients and 0.04 for the corresponding moment coefficients. Hence static coefficients may be equally well obtained using any of the specified instrument combinations. Comparison of the static force and moment coefficients in Figs. 5 and 6 show that very good agreement was obtained both between regions and with wind-tunnel data[10] when using the measurements from rate gyroscopes and four accelerometers. The results were generally within the same limits given previously.

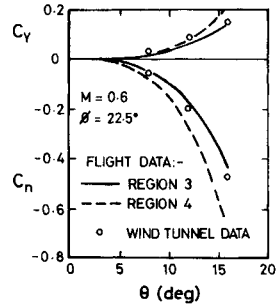

Fig. 6 Comparison of wind-tunnel and free-flight data, C_Y and C_n vs θ.

Magnus force and moment coefficients are not shown because of the large degree of uncertainty in their derivation. In addition, wind-tunnel tests[11] illustrate their high sensitivity and nonlinearity to a number of variations, both in the aerodynamic conditions and body configuration. Results for damping coefficient derivatives, which are also not given, showed reasonable consistency between different arrangements, but poor consistency between regions and with wind-tunnel data. Because the magnitude of the dynamic components is generally less than the error in the static coefficients, even approximate dynamic coefficients could not be expected to be derived. To obtain more accurate values, instrumentation accuracy must be improved and the dynamic components increased relative to the static ones.

Conclusions

Following each disturbance, the bomb experienced sufficient variation in θ, but limited variation in ϕ rendered the first two of four regions unsuitable for deriving aerodynamic coefficients. The two remaining flight regions produced static coefficients that agreed very well with each other as well as with corresponding wind-tunnel values. Satisfactory free-flight measurements of Magnus coefficients and damping coefficient derivatives were not obtained.

The very good agreement observed of values of q and r derived using rate gyroscope measurements compared with those derived using incidence meter data verified the rate gyroscope measurements and showed the accuracy of values derived from incidence meter data to be very good. In addition, the very good agreement observed of values of $\dot{q}$ and $\dot{r}$ derived using rate gyroscope measurements compared with those derived using accelerometer measurements indicated that aerodynamic coefficients could be determined using rate gyroscopes to replace two accelerometers without any significant loss in accuracy. In fact, static coefficients were equally well obtained using either four accelerometers only, rate gyroscopes and four accelerometers, or rate gyroscopes and each one of four possible combinations of two accelerometers.

References

[1] Rhodes, C. W. and Shannon, J. H. W., "Results and Conclusions of the Joint RAE/WRE Research Programme on the Flight Dynamics and Ballistic Consistency of Freely Falling Missiles, Part I—Bombs Stabilised by Fixed Cruciform Fins," TR HSA 20, Nov. 1965, Weapons Research Establishment, Salisbury, South Australia.

[2] Regan, F. J., Tanner, F. J., and Shannon, J. H. W., "Free-Fall Vehicle Dynamics Observation and Prediction," *Journal of Aircraft*, Vol. 7, No. 2, March-April 1970, pp. 141–144.

[3] Regan, F. J., Shannon, J. H. W., and Tanner, F. J., "Results and Conclusions of the Joint NOL/RAE/WRE Research Programme on the Free-Fall Dynamics of Bombs, Part II—A Low Drag Bomb with Split Skirt Stabilisers," TR HSA 26, Nov. 1969, Weapons Research Establishment, Salisbury, South Australia.

[4] Regan, F. J., Shannon, J. H. W., and Tanner, F. J., "Results and Conclusions of the Joint NOL/RAE/WRE Research Programme on the Free-Fall Dynamics of Bombs, Part III—A Low Drag Bomb with Freely Spinning Stabilisers," TR in preparation, Weapons Research Establishment, Salisbury, South Australia.

[5] Maple, C. G. and Synge, J. L., "Aerodynamic Symmetry of Projectiles," *Quarterly of Applied Mathematics*, Vol. 6, No. 4, Jan. 1949, pp. 345–366.

[6] Gilbert, N. E., "A Method for Deriving Aerodynamic Force and Moment Coefficients from Free Flight Data Using a Com-

puter Program," TN HSA 157, Oct. 1969, Weapons Research Establishment, Salisbury, South Australia.

[7] Gilbert, N. E., "Free Flight Measurement of Aerodynamic Lateral Force and Moment Coefficients on Bombs with Freely Spinning Cruciform and Monoplane Tails and Fixed Split Skirts," TN HSA 162, Nov. 1969, Weapons Research Establishment, Salisbury, South Australia.

[8] Gilbert, N. E., "The Use of Rate Gyroscopes in the Free Flight Measurement of Aerodynamic Lateral Force and Moment Coefficients," TN HSA 164, March 1970, Weapons Research Establishment, Salisbury, South Australia.

[9] Kolk, W. R., *Modern Flight Dynamics*, Space Technology Series, Prentice-Hall, Englewood Cliffs, N. J., 1961, pp. 6–11.

[10] Regan, F. J., Falusi, M. E., and Holmes, J. E., "Static Wind Tunnel Tests of the M823 Research Store with Fixed and Free-Spinning Tails," NOLTR 65-14, April 1967, U. S. Naval Ordnance Laboratory, White Oak, Silver Spring, Md.

[11] Regan, F. J., Holmes, J. E., and Falusi, M. E., "Magnus Measurements on the M823 Research Store with Fixed and Freely Spinning Cruciform Stabilizers, Freely Spinning Monoplane Stabilizers and Split-Skirt Stabilizers," NOLTR 69-214, Nov. 1969, U. S. Naval Ordnance Laboratory, White Oak, Silver Spring, Md.

Minimum Range-Sensitivity Deorbit

BARRY A. GALMAN*
RCA/Government and Commercial Systems, Camden, N. J.

Nomenclature

A = reference area for entry vehicle aerodynamic coefficients
C_D = entry vehicle drag coefficient
e = orbit eccentricity
h = altitude
L = angular momentum per unit mass
r = central radius
V = velocity
ΔV = retrovelocity impulse
W = entry vehicle weight
β = retrorocket alignment angle
γ = path angle (down from local horizontal)
η = true anomaly
θ = range angle from deorbit to entry
μ = planetary gravitational constant

Subscripts

o = initial unperturbed orbit condition
1 = condition immediately subsequent to retrofire
E = condition at atmospheric entry

Introduction

SINCE a principal contributer to the impact point dispersion of a deorbiting ballistic atmospheric entry vehicle is often retrorocket alignment error, the fact that a minimum range, minimum range-sensitivity alignment exists has long been of interest to designers of this type of spacecraft. Approximate equations describing this maneuver were published by Low[1] some years ago, showing that for a given retrovelocity ΔV, range dispersion is minimized (neglecting postentry atmospheric effects) when the retro-

Received September 14, 1970; revision received October 7, 1970. Much of the work for this paper was performed while the author was employed by the General Electric Co. Re-Entry and Environmental Systems Division. Programing support and other valuable assistance were provided by G. Keen of G. E.

* Staff Systems Manager, Plans and Systems Development. Member AIAA.

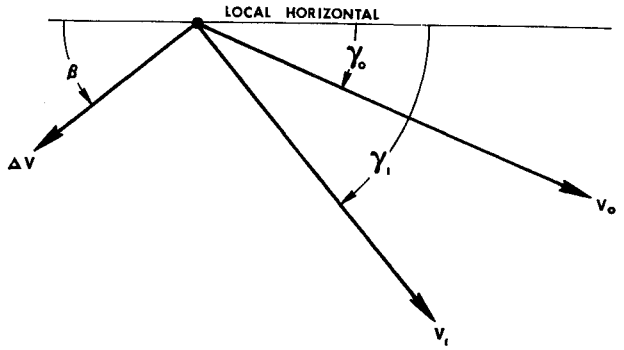

Fig. 1 Notation at deorbit point.

velocity vector is so aligned that $\partial\theta/\partial\beta = 0$. This maneuver may be contrasted to the minimum energy deorbit, of utility for lifting entry vehicles to minimize propulsion weight, where it is desired to achieve the steepest entry path angle possible for a given ΔV. An exact expression for the latter case has been developed previously,[2] and here a similar equation is presented for the minimum range-sensitivity deorbit which is also exact within the assumptions made and equally valid for elliptical orbits.

Analysis

In an inverse squared, drag-free force field, the basic conic orbit equation may be written in general as

$$1/r = 1 + e\cos\eta/(L^2/\mu) \tag{1}$$

Then the central radius at the atmospheric entry condition may be related to that immediately subsequent to retrofire by

$$1/r_E - 1/r_1 = (\mu e/L^2)(\cos\eta_E - \cos\eta_1) \tag{2}$$

Defining the range angle $\theta \equiv \eta_E - \eta_1$, Eq. (2) can be rewritten (following Cain[3]) by using the appropriate trigonometric formulas

$$1/r_E - 1/r_1 = -(\mu e/L^2)[\sin\eta_1 \sin\theta + \cos\eta_1(1 - \cos\theta)] \tag{3}$$

Now it is desirable to eliminate η_1 from the expression. Immediately from Eq. (1)

$$\cos\eta_1 = 1/e[(L^2/\mu r_1) - 1] \tag{4}$$

Furthermore, the path angle γ_1 may be expressed for a conic, and considering Fig. 1

$$\tan\gamma_1 = \frac{-e\sin\eta_1}{1 + e\cos\eta_1} = \frac{V_0\sin\gamma_0 + \Delta V\sin\beta}{V_0\cos\gamma_0 - \Delta V\cos\beta} \tag{5}$$

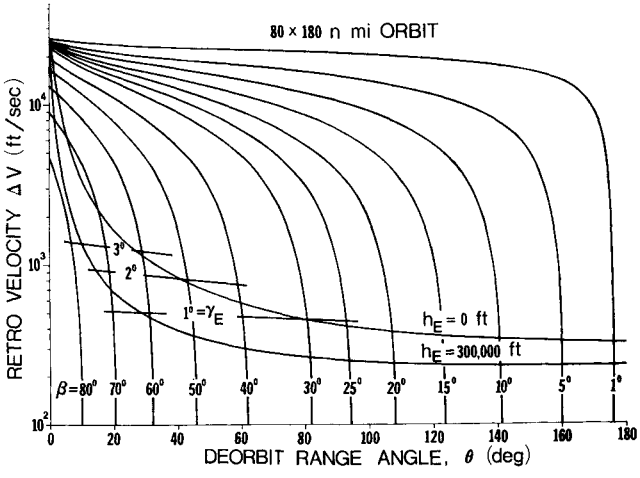

Fig. 2 Deorbit range angle vs ΔV, perigee deorbit.